Noname manuscript No.
(will be inserted by the editor)

Multi-dimensional Teager Kaiser and Higher Order Operators Based on Kronecker Power and Directional Derivatives

F. Salzenstein · A.O. Boudraa · T. Chonavel

Received: date / Accepted: date

Abstract This work aims at introducing some energy operators linked to Teager-Kaiser energy operator (Kaiser, 1990) and its associated higher order versions and expand them to multidimensional signals. These operators are very useful for analyzing oscillatory signals with time-varying amplitude and frequency (AM-FM). We prove that gradient tensors combined with Kronecker powers allow to express these operators by directional derivatives along any n-D vector. In particular, we show that the construction of a large class of non linear operators for AM-FM multidimensional signal demodulation is possible. Also, a new scalar function using the directional derivative along a vector giving the "sign" of the frequency components is introduced. An application of this model to local n-D AM-FM signal is presented and related demodulation error rates estimates. To show the effectiveness and the robustness of our method in term of envelope and frequency components extraction, results obtained on synthetic and real data are compared to multi-dimensional energy separation algorithm (Maragos and Bovik, 1995) and to our recently introduced n-D operator (Salzenstein and Boudraa, 2009).

Keywords Multidimensional Teager-Kaiser energy operator · Multi-dimensional Higher order differential operators · Kronecker product · Kronecker power · AM-FM Model · Directional derivative · Demodulation.

F. Salzenstein
Laboratoire INESS, UMR CNRS 7163 Université Strasbourg 1 (ULP), France.
Fax: +33 3 88 10 65 48
E-mail: salzenst@iness.c-strasbourg.fr

A.O. Boudraa
IRENav, Ecole Navale/Arts et ParisTech (EA 3634), BCRM Brest, CC 600, 29240 Brest, France.
E-mail: boudra@ecole-navale.fr

T. Chonavel
Lab-STICC, UMR 3192, TELECOM Bretagne, Technopole Brest Iroise, 29238 Brest, France.
E-mail: thierry.chonavel@telecom-bretagne.eu

1 Introduction

Teager-Kaiser Energy Operator (TKEO) (Kaiser, 1990) is a local energy tracking measure of oscillatory signals that is very easy to implement efficiently. In its continuous and 1-D version, TKEO computes the energy of a real-valued signal $x(t)$ as follows:

$$\Psi\left[s(t)\right] = [s^{(1)}(t)]^2 - s^{(0)}(t)s^{(2)}(t) \tag{1}$$

It has been shown that Ψ applied to an AM-FM signal $s(t) = a(t)\cos(\omega(t))$ can approximately estimate the squared product $a^2(t).\omega^2(t)$ assuming that $a(t)$ and $\omega(t)$ do not vary too fast or too greatly in time compared to the carrier frequency (Maragos et al, 1993a). Based on $\Psi\left[s(t)\right]$ a closed-formula for exact estimation of $a(t)$ and $\omega(t)$ called continuous Energy Separation Algorithm (ESA) is introduced (Maragos et al, 1993b). Even limited to narrow-band signals, TKEO is generally respecting the conditions of physical continuity required for the amplitude and the detected frequency (Vakman, 1996). For multi-component signals analysis, TKEO requires a bandpass filtering (Havlicek et al, 2005). TKEO has been extended to the bi-dimensional (2D) signals by Yu et al. (Yu et al, 1991). In images processing, this operator has been applied to demodulation (Maragos and Bovik, 1995), (Havlicek et al, 2005), (Boudraa et al, 2005), noise reduction (Vleesschauwer et al, 1997), image contrast enhancement (Mitra et al, 1991), (Ramponi et al, 1996), (Diop et al, 2008) and image thresholding (Boudraa et al, 2008). A 2D complex operator has also been developed to estimate the energy of oriented patterns (Larkin, 2005). Felsberg and Jonsson (Felsberg and Jonsson, 2005) have introduced energy tensors to describe the TKEO and expressed a gradient tensor by the means of the Kronecker product (Felsberg and Köthe, 2005). Moreover, higher order generalization of TKEO called k-order Differential Energy Operator (DEO) Ψ_k has been introduced by Maragos and Potamianos (Maragos and Potamianos, 1995):

$$\Psi_k\left[s(t)\right] = s^{(1)}(t)s^{(k-1)}(t) - s^{(0)}(t)s^{(k)}(t) \tag{2}$$

This class of operators is useful for demodulating AM-FM signals and for $k = 2$ we obtain the second-order differential energy operator.
We have extended these operators to the 2D continuous signals (Boudraa et al, 2005) and demonstrated their efficiency for surface roughness detection in white light interferometry (Salzenstein et al, 2005), providing a possible extension of the popular FSA method (Larkin, 1996). Moreover, a more general expression of TKEO and higher order operators for 1D signals has been recently introduced by the authors (Salzenstein et al, 2007). Recently, it has been shown the interest of such operators to separate multi-band components (Cai et al, 2010). Finally, we have also recently introduced a generalization of some previous operators to multi-dimensional signals by the means of higher order gradients and Kronecker products (Salzenstein and Boudraa, 2009). In particular, we have proved that the recurrence relation introduced in (Maragos and Potamianos, 1995) is effective at any dimension. A limit of these operators (Maragos and Potamianos, 1995),(Salzenstein and Boudraa, 2009) is their sensitivity in very noisy environment.

To overcome this problem, in this paper a new method that is robust against noise to compute the frequency components of a n-D signal by fixing the sign of each component is introduced. A new multi-dimensional scalar operator linking the directional derivatives and the gradients of a signal, including all partial derivatives at any order, is introduced in section 3 and the proofs of the theorem are reported into the appendix section. In section 4 we highlight the efficiency of our algorithm to demodulate local AM-FM signals provided that the scalar is proportional to a norm of the frequency vector. Thus we generalize the relations provided in (Maragos et al, 1993a), (Maragos and Bovik, 1995) to any n-D scalar model. A computation of the error under a such assumption has been performed (see appendix section). A new efficient scalar operator using a directional derivative along a vector containing the local "sign" frequency components is constructed. In section 5, the robustness against noise is shown and results compared to the multidimensional ESA (Maragos and Bovik, 1995) using synthetic and real data.

2 Multi-dimensional TKEO and higher-order tensors

Different operators extending TKEO to 2D signals have been developed (Maragos and Bovik, 1995), (Boudraa et al, 2005), (Larkin, 2005). These operators are useful for signal demodulation because their outputs are proportional to the square of the product of amplitude an frequency of the input 2D signal. For 2D signal $s(\mathbf{u})$, the introduced operators denoted respectively by Φ_B (Maragos and Bovik, 1995), Φ_C (Boudraa et al, 2005) and Φ_D (Larkin, 2005) can be expressed by an energy tensor $\Psi_t[s(\mathbf{u})]$ (Felsberg and Granlund, 2004) as follows:

$$\Psi_t[s(\mathbf{u})] = [\nabla s(\mathbf{u})][\nabla s(\mathbf{u})]^T - s(\mathbf{u}) H s(\mathbf{u}) = \begin{pmatrix} \Psi_{11} & \Psi_{12} \\ \Psi_{21} & \Psi_{22} \end{pmatrix}$$

where

$$\mathbf{u} = (x, y), \qquad \nabla s = \left[\frac{\partial s}{\partial x} \; \frac{\partial s}{\partial y} \right]^T, \qquad H = \nabla \nabla^T$$

∇ and H denote respectively the gradient and the Hessian of $s(\mathbf{u})$. We have the following relations:

$$\begin{aligned} \Phi_B[s(\mathbf{u})] &= \Psi_{11} + \Psi_{22} = \text{Trace}[\Psi_t[s(\mathbf{u})]] \\ \Phi_C[s(\mathbf{u})] &= \Psi_{11} + \Psi_{22} + \Psi_{12} + \Psi_{21} \\ \Phi_D[s(\mathbf{u})] &= \Psi_{11} - \Psi_{22} + j\Psi_{12} + j\Psi_{21} \end{aligned} \tag{3}$$

We have recently introduced (Salzenstein and Boudraa, 2009) a multi-dimensional approach extending both TKEO and k-order DEO. Let $\mathbf{u} = (x_1 \; x_2 \; ...x_n)$ be a n-D vector. For a multi-dimensional signal $s(\mathbf{u})$, the k^{th} order tensor denoted $\Psi_k[s(\mathbf{u})]$, is given by:

$$\Psi_k[s(\mathbf{u})] = \frac{ds}{d\mathbf{u}} \otimes \left(\frac{d^{k-1}s}{d\mathbf{u}^{k-1}} \right)^T - s \otimes \left(\frac{d^k s}{d\mathbf{u}^k} \right)^T \text{ for } k = 2p$$

$$\Psi_k[s(\mathbf{u})] = \frac{ds}{d\mathbf{u}} \otimes \left(\frac{d^{k-1}s}{d\mathbf{u}^{k-1}} \right) - s \otimes \left(\frac{d^k s}{d\mathbf{u}^k} \right) \text{ for } k = 2p+1$$

where symbol '$\otimes$' denotes the Kronecker product (Moon and Stirling, 2000). In particular, the trace of these tensors corresponds to Φ_B operator. A scalar operator $\Phi_k[s(\mathbf{u})]$ can be deduced by summing all elements of the matrix $\Psi_k[s(\mathbf{u})]$. Moreover, we have shown that this class of tensors enables to derive instantaneous envelope $A(\mathbf{u})$ and frequency vector $\mathbf{w} = (w_1\ w_2\ ...\ w_n)^T$ for any locally narrow band multi-dimensional signal such as:

$$s(x_1, x_2, ..., x_n) \simeq A(\mathbf{u}) \cos(\mathbf{w}\mathbf{u} + \theta)$$

In this case we are faced to the problem of recovering the sign of the instantaneous frequency signals as pointed out in (Maragos and Bovik, 1995). To resolve this problem, a new "sign" component solution has been proposed by the authors (Salzenstein and Boudraa, 2009). However, the proposed n-D method has two limits: a) it has been applied under local sinusoidal signal assumption and b) it can fail in presence of some frequency values. This paper deals with three main points: a) We give a general relation between the Kronecker powers and any higher order operators, b) we generalize the relations introduced in (Maragos et al, 1993a; Maragos and Bovik, 1995) related to the application of the mono dimensional and multi dimensional TK operators to any local n-D AM-FM signals and c) improve the robustness of the frequency estimation by the introduction of a new n-D scalar operator.

3 Generalization of TKEO by directional derivatives and Kronecker powers

In this section, a new multi-dimensional operator linking higher order scalar operators using directional derivatives and Kronecker powers is introduced. Thus the N-D problem is reduced to 1D one. Let $\Psi_{H_{k,p,m}}$ be a multi-dimensional tensor defined by:

$$\Psi_{H_{k,2p,2m+1}}[s(\mathbf{u})] = \frac{d^{2m+1}s}{d\mathbf{u}^{2m+1}} \otimes \left(\frac{d^{2l+1}s}{d\mathbf{u}^{2l+1}}\right)^T - \frac{d^{2p}s}{d\mathbf{u}^{2p}} \otimes \left(\frac{d^{2q}s}{d\mathbf{u}^{2q}}\right)^T \tag{4}$$

where $k = 2p + 2q = 2m + 1 + 2l + 1$ for an even order tensor.

$$\Psi_{H_{k,2p,2m+1}}[s(\mathbf{u})] = \frac{d^{2m+1}s}{d\mathbf{u}^{2m+1}} \otimes \left(\frac{d^{2l}s}{d\mathbf{u}^{2l}}\right) - \frac{d^{2p}s}{d\mathbf{u}^{2p}} \otimes \left(\frac{d^{2q+1}s}{d\mathbf{u}^{2q+1}}\right) \tag{5}$$

where $k = 2p + 2q + 1 = 2m + 2l + 1\ \ (m, l) \neq (p, q)$ for an odd order tensor. This corresponds to a multidimensional generalization of operators introduced in (Salzenstein et al, 2007). According to Kronecker product properties, dimen-

sions of the matrices are given as follows:

$$\begin{aligned}
\frac{d^{2p}s}{d\mathbf{u}^{2p}} &\Rightarrow n^p \text{ rows } \times n^p \text{ columns} \\
\frac{d^{2q}s}{d\mathbf{u}^{2q}} &\Rightarrow n^q \text{ rows } \times n^q \text{ columns} \\
\frac{d^{2m+1}s}{d\mathbf{u}^{2m+1}} &\Rightarrow n^m \text{ rows } \times n^{m+1} \text{ columns} \\
\frac{d^{2l+1}s}{d\mathbf{u}^{2l+1}} &\Rightarrow n^l \text{ rows } \times n^{l+1} \text{ columns}
\end{aligned}$$

Then it follows immediately from Eq. (4) and (5), that $\Psi_{H_{k,2p,2m+1}}$ is a $n^{m+l+1} \times n^{m+l+1} = n^{p+q} \times n^{p+q}$ matrix when k is an even integer and a $n^{m+l} \times n^{m+l+1} = n^{p+q} \times n^{p+q+1}$ matrix when k is an odd integer.
Let us now use the "Kronecker power" of any $n \times 1$ vector $\mathbf{v} \in \mathbb{R}^n$ (Vetter, 1973):

$$\bigotimes_p \mathbf{v} = \mathbf{v} \otimes \mathbf{v} \otimes ... \otimes \mathbf{v} \tag{6}$$

This gives a $n^p \times 1$ vector. The following proposition provides the relationship between higher order tensors and higher order directional derivatives

Proposition 1 *Link between higher order even tensor (Eq. 4) and all directional derivatives is given by:*

$$(\bigotimes_{p+q} \mathbf{v}^{\mathbf{T}})\Psi_{H_{k,2p,2m+1}}[s(\mathbf{u})](\bigotimes_{p+q} \mathbf{v}) = \frac{\partial^{2m+1}s}{\partial \mathbf{v}^{2m+1}} \left(\frac{\partial^{2l+1}s}{\partial \mathbf{v}^{2l+1}}\right)^T - \frac{\partial^{2p}s}{\partial \mathbf{v}^{2p}} \left(\frac{\partial^{2q}s}{\partial \mathbf{v}^{2q}}\right)^T \tag{7}$$

In the same way, a link between higher order odd tensor (Eq. 5) and all directional derivatives is given by:

$$(\bigotimes_{p+q} \mathbf{v}^{\mathbf{T}})\Psi_{H_{k,2p,2m+1}}[s(\mathbf{u})](\bigotimes_{p+q+1} \mathbf{v}) = \frac{\partial^{2m+1}s}{\partial \mathbf{v}^{2m+1}} \left(\frac{\partial^{2l}s}{\partial \mathbf{v}^{2l}}\right)^T - \frac{\partial^{2p}s}{\partial \mathbf{v}^{2p}} \left(\frac{\partial^{2q+1}s}{\partial \mathbf{v}^{2q+1}}\right)^T \tag{8}$$

See the complete proof of the theorem in appendix A and B. According to Eqs. (7)-(8) it is possible to construct a large class of scalar operators based on a large class of higher order tensors Ψ_{H_k} choosing different vectors $\mathbf{v}$.
Let us denote respectively $\Phi_{H_{k,2p,2m+1}}[s(\mathbf{u})]$ and $\Phi_{H_{k,2p,2m+1}}[s(\mathbf{u})]$ the previous operators. For example, the scalar defined in (Salzenstein and Boudraa, 2009) corresponds to a $n \times 1$ vector $\mathbf{v} = \begin{pmatrix} 1 & ... & 1 \end{pmatrix}^T$:

$$\Phi_{2p}[s(\mathbf{u})] = (\bigotimes_p \mathbf{v}^{\mathbf{T}})\Psi_{2p}[s(\mathbf{u})](\bigotimes_p \mathbf{v}) \tag{9}$$

$$\Phi_{2p+1}[s(\mathbf{u})] = (\bigotimes_p \mathbf{v}^{\mathbf{T}})\Psi_{2p}[s(\mathbf{u})](\bigotimes_{p+1} \mathbf{v}) \tag{10}$$

The particular case of the second order operator gives the directional TKEO, which extends the 1D classical TKEO to the directional derivatives along any unit vector:

$$\mathbf{v}^T \Psi_2[s(\mathbf{u})]^T \mathbf{v} = \left(\frac{\partial s}{\partial \mathbf{v}}(\mathbf{u})\right)^2 - s(\mathbf{u})\frac{\partial^2 s}{\partial \mathbf{v}^2}(\mathbf{u}) \tag{11}$$

In the next sections we use the following notation: TKEO scalar operator associated with the vector $\mathbf{v}$ and tensor $\Psi_2[s(\mathbf{u})]$ is denoted $\Phi_{2,\mathbf{v}}[s(\mathbf{u})]$ i.e:

$$\mathbf{v}^T \Psi_2[s(\mathbf{u})]^T \mathbf{v} = \Phi_{2,\mathbf{v}}[s(\mathbf{u})] \tag{12}$$

As it will be seen in the next section, an interesting application of this method is the efficient AM-FM signal demodulation.

4 Demodulation of n-D signal

In this section, an envelope and frequency demodulation method of any local AM-FM signal (section 4.1) is presented. In particular, the general condition related to the choice of a directional derivative, which leads to a new stable and robust method (section 4.2) is provided.

4.1 Instantaneous envelope and frequency demodulation

Let s be an n-dimensional an AM-FM signal defined by:

$$s(\mathbf{u}) = A(\mathbf{u}) \cos\left(\phi(\mathbf{u})\right)$$

The signal must have smooth local coherency in order to ensure a particular pair of AM-FM components can be selected (Bovik et al, 1992). When the envelop $A(\mathbf{u})$ does not vary too fast compared to the carrier, the gradient of the phase is such that $\nabla\phi = \mathbf{w}(\mathbf{u}) \simeq \mathbf{w}$, the local frequency vector is given by $\mathbf{w} = (w_1\ w_2\ ...\ w_n)^T$. We choose a normalized vector $\mathbf{v} = (v_1\ v_2\ ...\ v_n)^T$ such that (see next section):

$$\frac{\partial \phi}{\partial \mathbf{v}} = \frac{d\phi}{d\mathbf{u}}\mathbf{v} = \mathbf{w}^T\mathbf{v} \geq ||w|| \tag{13}$$

This assumption leads to the following approximation (see also appendix C):

$$\Phi_{2,\mathbf{v}}[s(\mathbf{u})] \simeq A(\mathbf{u})^2 \left(\frac{\partial \phi}{\partial \mathbf{v}}(\mathbf{u})\right)^2 = A(\mathbf{u})^2 \left(\mathbf{w}(\mathbf{u})^T\mathbf{v}\right)^2 \tag{14}$$

Then, the extracted envelope is given by

$$A(\mathbf{u})^2 \simeq \frac{\left|\Phi^2_{2,\mathbf{v}}[s(\mathbf{u})]\right|}{\left|\Phi^2_{2,\mathbf{v}}[\frac{\partial s(\mathbf{u})}{\partial \mathbf{v}}]\right|} = \frac{\left|\Phi^2_{2,\mathbf{v}}[s(\mathbf{u})]\right|}{\left|\Phi^2_{4,\mathbf{v}}[s(\mathbf{u})]\right|} \tag{15}$$

Hence, Eq. (7) is helpful to compute the scalar $\Phi^2_{4,\mathbf{v}}[s(\mathbf{u})]$. Such result can be easily extended to any higher order operators and computed by using Eqs. (7)-(8). The instantaneous frequency vector components are estimated generalizing the algorithm developed in (Salzenstein and Boudraa, 2009).
Let us consider $s_{i_1x_1,i_2x_2,...,i_nx_n}(\mathbf{u})$ obtained by the partial derivatives along x_i.

$$s_{i_1x_1,i_2x_2,...,i_nx_n}(\mathbf{u}) = i_1\frac{\partial s}{\partial x_1} + i_2\frac{\partial s}{\partial x_2} + ... + i_n\frac{\partial s}{\partial x_n} \tag{16}$$

where i_j are integers. One can write using (15):

$$(i_1 w_1 + i_2 w_2 + ... + i_n w_n)^2 \simeq \frac{\Phi_{2,\mathbf{v}}[s_{i_1 x_1, i_2 x_2, ..., i_n x_n}(\mathbf{u})]}{\Phi_{2,\mathbf{v}}[s(\mathbf{u})]} \tag{17}$$

As in (Salzenstein and Boudraa, 2009) it is then possible to extract a *unique* frequency vector. We call $\mathbf{w^{(j)}} = (w_1^{(j)} \ ... \ w_n^{(j)})$ the set of components obtained fixing the sign $\epsilon_j = \pm 1$ of a chosen component $w_j = \epsilon_j |w_j| (\neq 0)$:

1. Compute the quantities:

$$|w_j| = \sqrt{\frac{\Phi_{2,\mathbf{v}}[s_{x_j}]}{\Phi_{2,\mathbf{v}}[s]}} \tag{18}$$

$$w_j w_k = \frac{\Phi_{2,\mathbf{v}}[s_{x_j} + s_{x_k}] - \Phi_{2,\mathbf{v}}[s_{x_j} - s_{x_k}]}{4\Phi_{2,\mathbf{v}}[s]} \tag{19}$$

2. Compute the jth component:

$$w_j^{(j)} = \epsilon_j \text{sign}\,(w_j w_j)\,|w_j| = \epsilon_j |w_j|$$

3. Compute of the kth component, $k \in \{1, ..., n\}$:

$$w_k^{(j)} = \epsilon_j \text{sign}\,(w_k w_j)\,|w_k|$$

4.2 Choice of the directional derivatives

The recent model introduced in (Salzenstein and Boudraa, 2009) corresponds to the directional derivatives along the vector $\mathbf{v} = (1, 1, ..., 1)^T$. However, this algorithm can fail when the sum of the frequency components is null:

$$\mathbf{w}^T \mathbf{v} = w_1 + w_2 + ... + w_n = 0$$

To ensure the stability of the method, condition (20) is necessary :

$$\Phi_{2,\mathbf{v}}[A(\mathbf{u}) \cos(\mathbf{w}\mathbf{u} + \theta)] = 0 \Leftrightarrow \mathbf{w} \simeq \mathbf{0} \tag{20}$$

We have added a second condition in order to minimize the error bound:

$$\frac{\partial \phi}{\partial \mathbf{v}} = \frac{d\phi}{d\mathbf{u}} \mathbf{v} = \mathbf{w}^T \mathbf{v} \geq ||w|| \tag{21}$$

In other words, any local AM-FM signal applied to a generalized scalar operator $\Phi_{2,\mathbf{v}}[s(\mathbf{u})]$ should be proportional or greater to a norm of the frequency vector. The image demodulation technique developed in (Maragos and Bovik, 1995) corresponds to the usual Euclidean quadratic norm. In this paper, we propose a new scalar multi-dimensional algorithm which is compared favorably to the previous ones, using local directional derivatives according to the normalized vector

$$\mathbf{v}(\mathbf{u}) \propto \text{sign}(\mathbf{w}) = (\text{sign}(w_1) \ \text{sign}(w_2) \ ... \ \text{sign}(w_n))^T$$

at any point $\mathbf{u}$. Applying Eq. (14) leads immediately to:

$$\Phi_{2,\text{sign}(\mathbf{w})}[s\,(\mathbf{u})] \simeq \frac{A^2}{n} (\sum |w_i|)^2 \tag{22}$$

The main problem lies in the recovering of the sign of the local frequency components. To overcome this problem, calculus of Eq. (22) is done in another way. Actually, the general term of the matrix $\Psi_2[s(\mathbf{u})]$ computed by the relation (4) equals:

$$[\Psi]_{ij} \simeq A^2 w_i^{k_i} w_j^{k_j} \qquad k_i + k_j = 2 \tag{23}$$

Thus summing all absolute values of the elements of the matrix provide the final expression:

$$\sum_{i,j} \left|[\Psi]_{ij}\right| = A^2 \left(|w_1 + ... + |w_n|\right)^2 \tag{24}$$

which is proportional to the general scalar operator (22) using a directional derivative along the vector $\mathbf{v}(\mathbf{u}) = (\text{sign}(w_1)\ \text{sign}(w_2)\ ...,\ \text{sign}(w_n))^T$ at any point $\mathbf{u}$. Finally we apply the general algorithm in order to demodulate local AM-FM signal:

1. Compute the matrix $\Psi_{H_{k,2p,2m+1}}[s(\mathbf{u})]$ using the relation (4) for an even order $k = 2$ (resp. $k = 4$) and the associated parameters p, q, m, l (resp. $p1, q1, m1, l1$) provided that $k = 2p + 2q = 2m + 1 + 2l + 1$ (resp. $2k = 2p1 + 2q1 = 2m1 + 1 + 2l1 + 1$)
2. Compute the sum of all absolute values of the elements of the matrix;
3. Compute the instantaneous envelope using Eq. (15);
4. Compute the instantaneous frequency components using the "sign" algorithm outlined at the end of the subsection 4.1;

This algorithm corresponding to the operator $\Psi_{2,\text{sign}(\mathbf{w})}$ is called **Algo 1**.

4.3 An alternative algorithm using eigenvectors

Moreover, we will show in this section that there is an alternative way to compute the sign of the frequency components. Actually the general term of the tensor matrix Ψ_2 approximatively equals to $A^2 w_i w_j$ where w_i and w_j are respectively the ith and jth component of the frequency vector (i.e, the gradient of the phase). It is immediate to observe that the normalized frequency vector:

$$\mathbf{v} = \frac{\mathbf{w}}{||\mathbf{w}||}$$

remains an eigenvector associated with the eigenvalue $\lambda = A^2||\mathbf{w}||^2$. Although this eigenvector does not provide the absolute frequency vector, it provides the relative sign of the frequency components, i.e the local orientation. On the other hand, Ψ_2 is a symmetric matrix, which defines a positive semi-definite quadratic form for any narrow band signal i.e:

$$\forall \mathbf{v} \neq \mathbf{0} \quad \mathbf{v}^T \Psi_2[s]\mathbf{v} \geq 0$$

According to the properties of such forms, it follows that its eigenvalues are positive or null (Moon and Stirling, 2000). Moreover, the trace of the tensor equals $A^2||\mathbf{w}||^2$ it follows immediately that $\lambda = A^2||\mathbf{w}||^2$ corresponds to the maximum eigenvalue of Ψ_2 (the two other eigenvalues being null, showing that the tensor is a singular matrix). Thus instead of the step 4 in Algo 1, we propose the following algorithm in order to compute the frequency vector:

1. Compute the quantities:

$$|w_j| = \sqrt{\frac{\Phi_{2,\mathbf{v}}[s_{x_j}]}{\Phi_{2,\mathbf{v}}[s]}} \tag{25}$$

2. Compute the eigenvector $\mathbf{v}$ of the tensor Ψ_2 associated with its maximum eigenvalue.
3. compute of the jth component, $j \in \{1, ..., n\}$:

$$w_j = \text{sign}\,(v_j)\,|w_j|$$

This algorithm is referred as **Algo 2**. This step only focus on the frequency estimation, for the envelope detection being the procedure is identical to **Algo 1**. Let us remark that the scalar operator $\Phi_{2,\mathbf{v}}$ associated with the eigenvector $\mathbf{v}$ provides the trace of Ψ_2 i.e, an operator which is comparable to Φ_B.

5 Results and discussions

To show the efficiency of our method, the results on synthetic and real data are compared to our previous operator Φ_k (Salzenstein and Boudraa, 2009) and the classical n-D operator Φ_B introduced by Maragos et Bovik (Maragos and Bovik, 1995). This operator corresponds to the trace of the Ψ_2 tensor. The output of Φ_B to a $n-$dimensional AM-FM signal with slowly varying amplitude and frequencies is given by (Maragos and Bovik, 1995):

$$\Phi_B[s(\mathbf{u})] = A^2 \left(w_1^2 + w_2^2 + ... + w_n^2\right) \tag{26}$$

For narrow band AM-FM signal the envelope and the the modulus of the frequency components can be approximated by the following relations:

$$A^2 \approx \frac{\Phi_B[s(\mathbf{u})]}{\sum_{k=1}^{n} \Phi_B[s_{x_k}]} \qquad (w_k)^2 \approx \frac{\Phi_B[s_{x_k}]}{\Phi_B[s(\mathbf{u})]}$$

Thus, Φ_B based demodulation requires derivatives until the third order. While operator Φ_k (Salzenstein and Boudraa, 2009) requires partial derivatives until the forth order, the new multi-dimensional scalar operator (Eq. 4) is calculated for respective orders $k = 2$ and $k = 4$ (Step 1 of section 4.2). These functions also require derivatives until the third order. Note that, although in (Maragos and Bovik, 1995) the problem of relative sign of the frequency components has not been studied, a possible solution to this problem is to replace $\Psi_{2,\mathbf{v}}$ by Φ_B in equations (25) and (19). We compare **Algo 1** and **Algo 2** to Φ_B and Φ_k operators on 2D and 3D data in term of instantaneous envelope and frequency components extraction. Comparison with other multi-dimensional methods have been reported in (Salzenstein and Boudraa, 2009) where the 3D approaches i.e, the algorithms Φ_B and Φ_k give best results. The relative error rates related to the original data (if available) are calculated at each point $\mathbf{u} = (x\ y\ z)$ as follows:

$$\varepsilon_{env} = \frac{|A(\mathbf{u}) - \hat{A}(\mathbf{u})|}{A(\mathbf{u})} \qquad \varepsilon_{freq} = \frac{||\mathbf{w}(\mathbf{u}) - \hat{\mathbf{w}}(\mathbf{u}||}{||\mathbf{w}(\mathbf{u})||}$$

Different slices of a synthetic fringe pattern (128 x 128 x 128) where the envelope and the local carrier waves are varying according to the directions and magnitudes of the frequency vectors are presented in figures 1 and 2. Error rates of envelope and frequency estimates given by all methods for the two synthetic data in noise free and noisy environments are summarized in tables 1-6. Tables 1-2 report the results for noise free data while tables 3-4 and tables 5-6 summarize the results with respective noise levels of 10% and 20%. Globally, the new operator $\Psi_{2,\mathrm{sign}(\mathbf{w})}$ (**Algo 1**) gives a better error rate than the other multi-dimensional energy separation algorithms. The improvement in frequency detection in noisy environment, is particularly interesting as illustrated by the results reported by table 6. In a 3D noisy context, the frequency detection using the eigenvector (**Algo 2**) give the worst error rates. Other experimental results performed on 2D real data in both noisy and free noise context confirm the high performance of the method $\Psi_{2,\mathrm{sign}(\mathbf{w})}$ (**Algo 1**) regarding the local frequency detection. Actually, figures 3,4 illustrate the frequency component detection in a context of a noisy/free noise images. Sonar images and fingerprint patterns (extracted from the database[1]) are represented in Figs. 3,4. Sonar images show ripples and ridges of sand where their orientation and frequency oscillations are very useful informations for sea-bed characterization. We have focused on the quantitative performances of the operators related to the frequency components. The frequency vectors extracted by Φ_B is more visually degraded specifically in the noisy context (see Fig. 3(c) and (f), 4(e) and (f). Tables 7 and 8 also summarize the quantitative results corresponding to the relative error rates between the frequency detection in the free noise context and the one in the noisy context, for different levels of noise. In all cases the new algorithm $\Psi_{2,\mathrm{sign}(\mathbf{w})}$-**Algo 1** and even $\Psi_{2,\mathrm{sign}(\mathbf{w})}$-**Algo 2** show their effective robustness, providing good error rates. As we have chosen a unique reference for the comparison with the free noise context ($\Psi_{2,\mathrm{sign}(\mathbf{w})}$ (**Algo 1**) or Φ_B) or a reference with regard to each algorithm, the levels of error rates remain the unchanged.

6 Conclusion

In this paper, a generalization of TKEO and higher order differential operators to multi-dimensional signals using higher order gradients combined with Kronecker product is introduced. In particular we have highlighted the link between these tensors and any directional derivatives along a vector, which allows to construct a large class of functions. An appropriate choice of the directional vector leads to operators which are proportional to a quadratic norm of the frequency. An important aspect of our algorithm is the ability to demodulate local AM-FM signals. A new scalar operator corresponding to a directional derivative along the vector containing the "sign" of the frequency vector has been introduced. A comparison with some multi-dimensional energy separation algorithms shows the competitiveness and robustness of our approach to estimate the instantaneous envelope and frequency components.

[1] http://bias.csr.unibo.it/fvc2000/download.asp

7 Figures and tables

Table 1 Global envelope error rates for noise-free patterns

Operators	Contrast Pattern I (Fig. 1)	Contrast Pattern II (Fig. 2)
3D $\Phi_{2,\mathrm{sign}(\mathbf{w})}$	1.73%	0.16%
D Φ_k	1.73%	0.49%
3D Φ_B	2.22%	0.32%

Table 2 Global frequency error rates noise-free patterns

Operators	Contrast. pattern I	Contrast pattern II
3D $\Phi_{2,\mathrm{sign}(\mathbf{w})}$ - Algo 1	2.61%	3.48%
3D $\Phi_{2,\mathrm{sign}(\mathbf{w})}$ - Algo 2	2.61%	6.54%
3D Φ_k	2.63%	3.48%
3D Φ_B	2.63%	3.48%

Table 3 Global envelope error rates for 10 % noisy patterns

Operators	Contrast Pattern I (Fig. 1)	Contrast Pattern II (Fig. 2)
3D $\Phi_{2,\mathrm{sign}(\mathbf{w})}$	8.29%	6.39%
3D Φ_k	7.61%	6.48%
3D Φ_B	9.27%	6.62%

Table 4 Global frequency error rates for 10 % noisy patterns

Operators	Contrast. pattern I	Contrast pattern II
3D $\Phi_{2,\mathrm{sign}(\mathbf{w})}$ - Algo 1	3.25%	3.57%
3D $\Phi_{2,\mathrm{sign}(\mathbf{w})}$ - Algo 2	13.24%	8.24%
3D Φ_k	4.42%	3.93%
3D Φ_B	4.38%	3.72%

Table 5 Global envelope error rates for 20 % noisy patterns

Operators	Contrast Pattern I (Fig. 1)	Contrast Pattern II (Fig. 2)
3D $\Phi_{2,\mathrm{sign}(\mathbf{w})}$	14.13%	12.15%
3D Φ_k	13.96%	12.51%
3D Φ_B	16.09%	12.84%

Table 6 Global frequency error rates for 20 % noisy patterns

Operators	Contrast. pattern I	Contrast pattern II
3D $\Phi_{2,\mathrm{sign}(\mathbf{w})}$ - Algo 1	4.98%	3.95%
3D $\Phi_{2,\mathrm{sign}(\mathbf{w})}$ - Algo 2	13.8%	8.21%
3D Φ_k	12.81%	6.72%
3D Φ_B	10.01%	5.12%

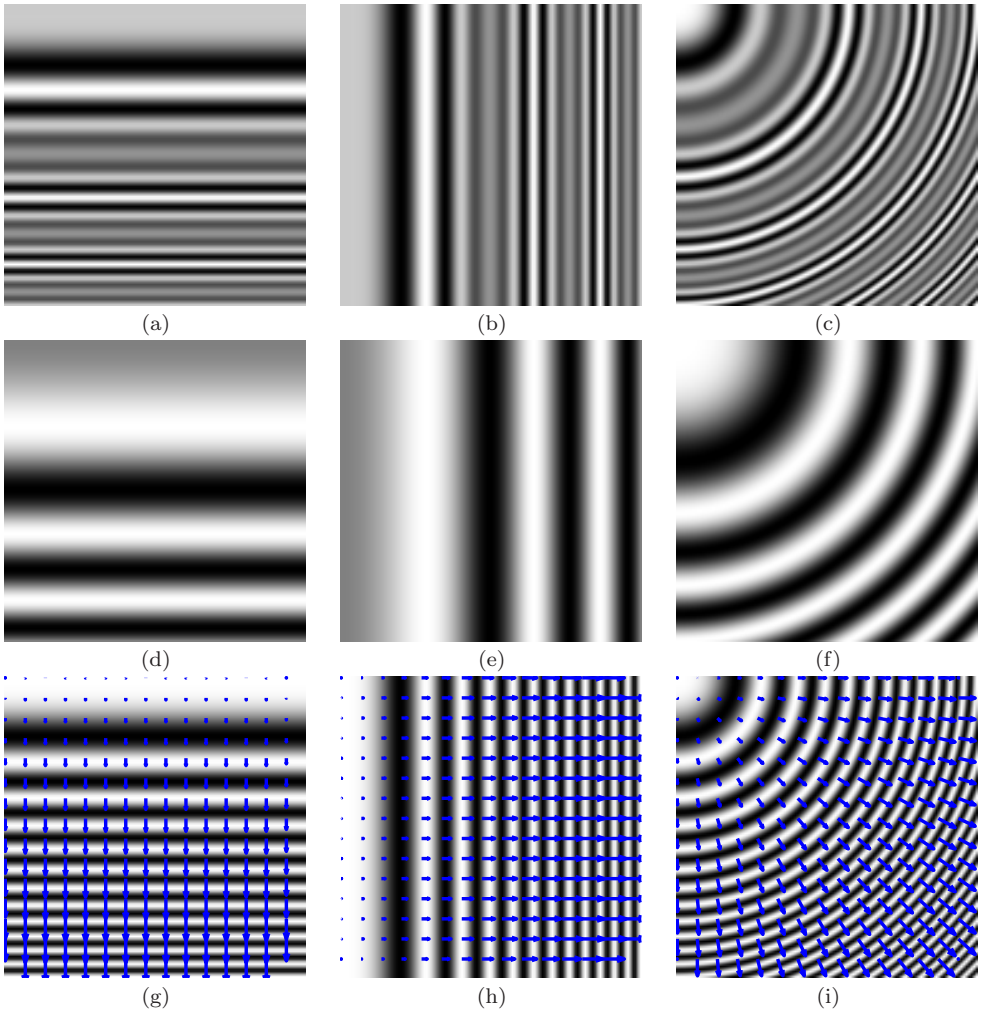

Fig. 1 Contrasted pattern (I) with a contrasted envelope. (a) xy slice; (b) yz slice; (c) xz slice; (d) xy envelope; (e) yz envelope; (f) xz envelope; (g) xy frequency and carrier; (h) yz frequency and carrier; (i) xz frequency and carrier

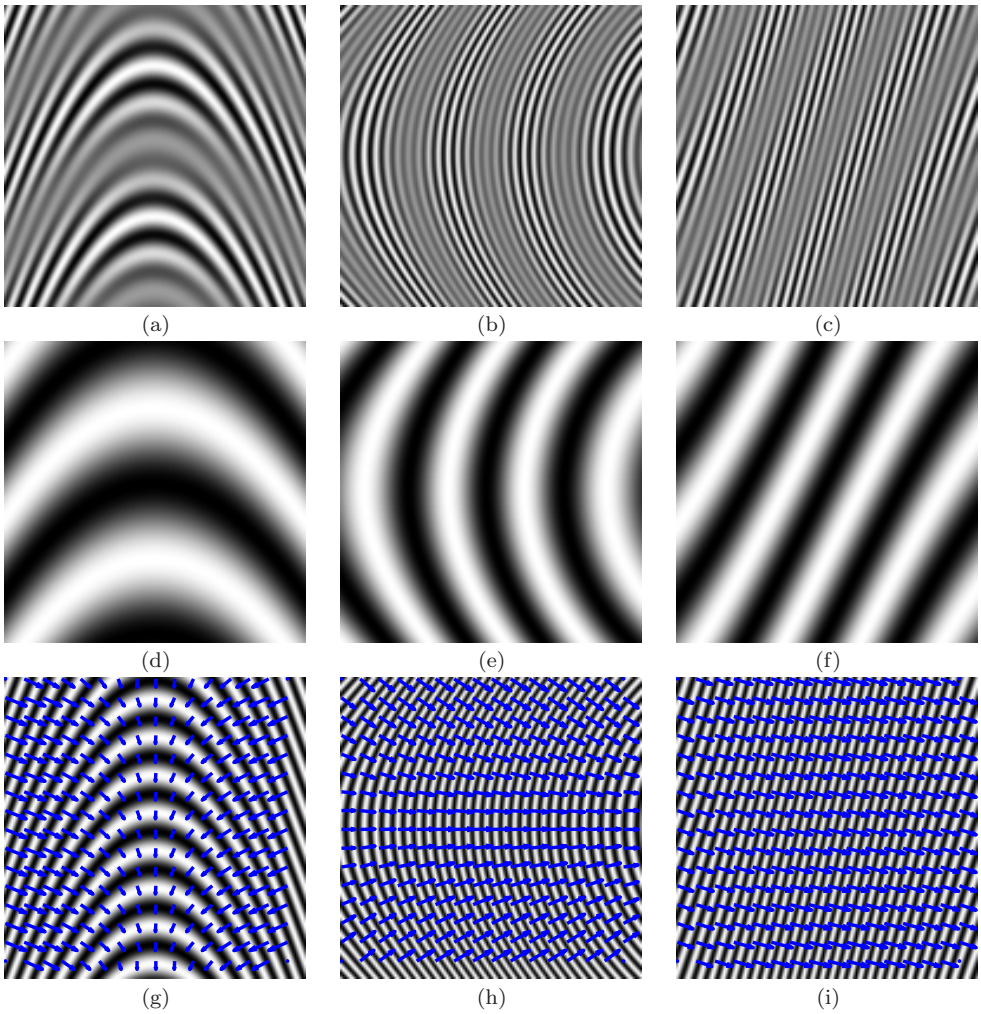

Fig. 2 Contrasted pattern (II) with a contrasted envelope. (a) xy slice; (b) yz slice; (c) xz slice; (d) xy envelope; (e) yz envelope; (f) xz envelope; (g) xy frequency and carrier; (h) yz frequency and carrier; (i) xz frequency and carrier

Table 7 Global frequency error rates for 10 % noisy patterns

Operators	Interferometric Image	Sonar Image	Fingerprint
2D $\Phi_{2,\mathrm{sign}(\mathbf{w})}$ - Algo 1	6.24%	3.67%	2.53%
2D $\Phi_{2,\mathrm{sign}(\mathbf{w})}$ - Algo 2	6.22%	2.97%	1.80%
2D Φ_k	19.41%	9.73%	8.07%
2D Φ_B	14.82%	12.58%	7.94%

Table 8 Global frequency error rates for 20 % noisy patterns

Operators	Interferometric Image	Sonar Image	Fingerprint
2D $\Phi_{2,\mathrm{sign}(\mathbf{w})}$ - Algo 1	7.11%	5.98%	4.97%
2D $\Phi_{2,\mathrm{sign}(\mathbf{w})}$ - Algo 2	7.19%	5.52%	4.54%
2D Φ_k	22.91%	14.86%	13.82%
2D Φ_B	16.74%	14.97%	18.64%

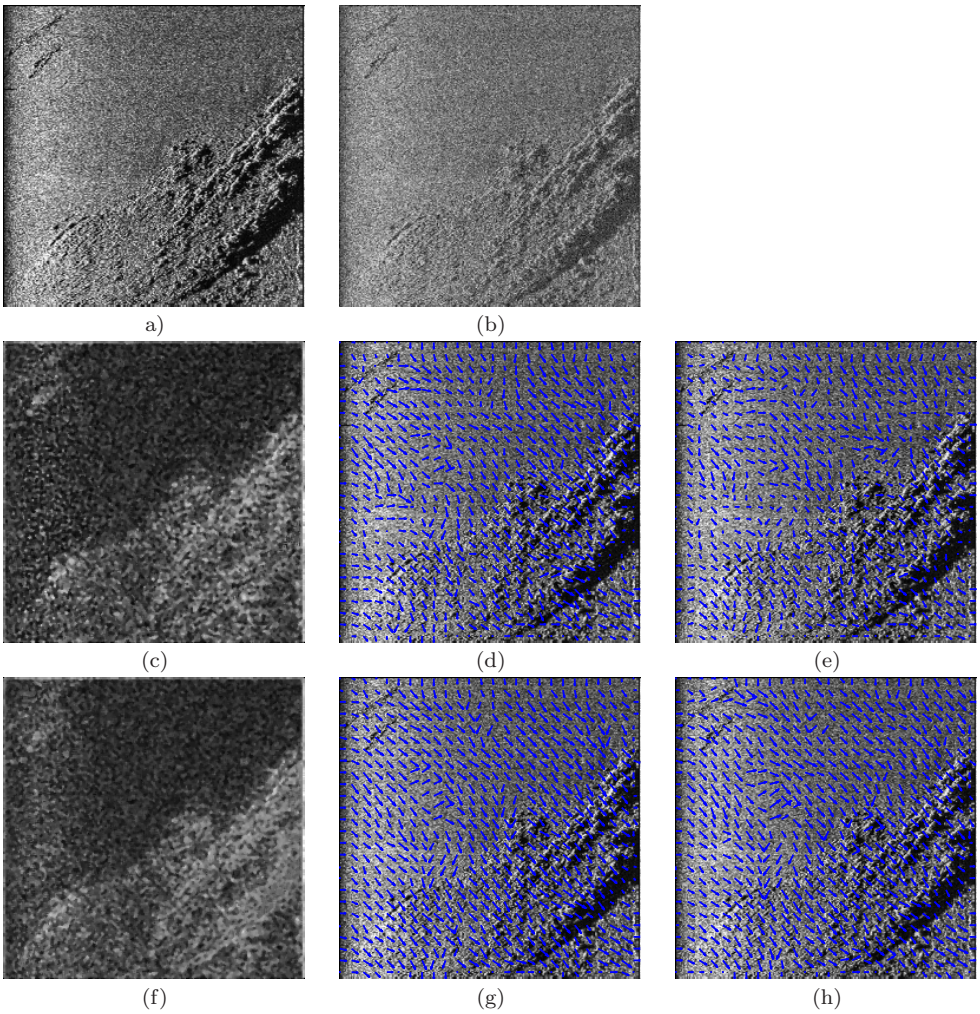

Fig. 3 Sonar image. (a) free noise original slice; (b) 20% noisy original image; (c) estimated envelope by Φ_B; (d) free noise estimated frequency by Φ_B; (e) 20% noisy estimated frequency by Φ_B; (f) estimated envelope by Φ_{H_k} ; (g) free noise estimated frequency by Φ_{H_k}; (h) 20% noisy estimated frequency by Φ_{H_k}

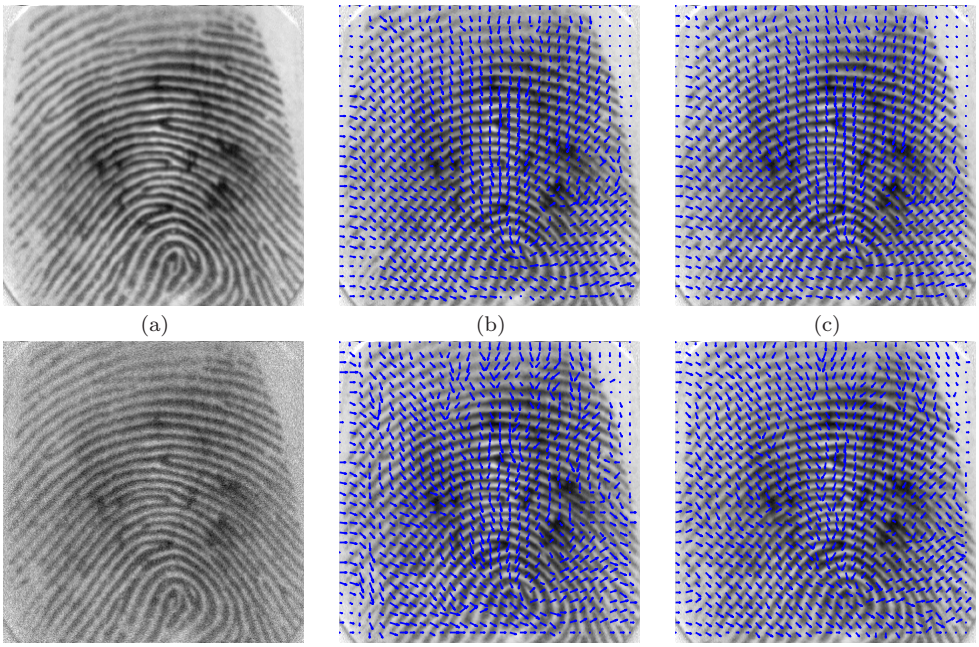

(a) (b) (c)

(d) (e) (f)

Fig. 4 Fingerprints: (a) original image; (b) estimated frequency by Φ_B; (c) estimated frequency by Φ_{H_k}; (d) noisy image; (e) estimated frequency by Φ_B; (f) estimated frequency by Φ_{H_k};

Appendix

A Relation between higher order gradients and directional derivatives using Kronecker product

The derivative of a product $\mathbf{AB}$ yields:

$$\begin{aligned}\frac{d}{d\mathbf{u}}(\mathbf{AB}) &= \left(\frac{\partial(\mathbf{AB})}{\partial x_1} \ \ldots \ \frac{\partial(\mathbf{AB})}{\partial x_n}\right)\\ &= \left(\frac{\partial \mathbf{A}}{\partial x_1}\mathbf{B} + \mathbf{A}\frac{\partial \mathbf{B}}{\partial x_1} \ \ldots \ \frac{\partial \mathbf{A}}{\partial x_n}\mathbf{B} + \mathbf{A}\frac{\partial \mathbf{B}}{\partial x_n}\right)\\ &= \left(\frac{\partial \mathbf{A}}{\partial x_1} \ \ldots \ \frac{\partial \mathbf{A}}{\partial x_n}\right)\begin{pmatrix}\mathbf{B} & \mathbf{0} & \ldots & \mathbf{0}\\ \mathbf{0} & \mathbf{B} & \ldots & \mathbf{0}\\ \mathbf{0} & \ldots & \mathbf{0} & \mathbf{B}\end{pmatrix}\\ &+ \mathbf{A}\left(\frac{\partial \mathbf{B}}{\partial x_1} \ \ldots \ \frac{\partial \mathbf{B}}{\partial x_n}\right)\\ &= \frac{d\mathbf{A}}{d\mathbf{u}}(\mathbf{I_n}\otimes\mathbf{B}) + \mathbf{A}\frac{d\mathbf{B}}{d\mathbf{u}}\end{aligned} \tag{27}$$

Where $\mathbf{I_n}$ represents the **identity** matrix $\mathbf{n}\times\mathbf{n}$. A general result dealing with derivatives according to a matrix (instead of a vector) can be found in (Brewer, 1978). In particular, we derive the following properties, where $\mathbf{v}$ and $\mathbf{w}$ represent any constant vectors, provided that the dimensions are compatible:

$$\frac{d}{d\mathbf{u}}(\mathbf{vAw}) = \mathbf{v}\frac{d\mathbf{A}}{d\mathbf{u}}(\mathbf{I_n}\otimes\mathbf{w}) \tag{28}$$

Moreover, a property of the Kronecker product (Moon and Stirling, 2000) yields:

$$(\mathbf{A} \otimes \mathbf{B})(\mathbf{C} \otimes \mathbf{D}) = (\mathbf{AC}) \otimes (\mathbf{BD}) \tag{29}$$

We deduce, provided that the dimensions are compatible:

$$\begin{aligned} &(\mathbf{A_1} \otimes \mathbf{B_1})(\mathbf{A_2} \otimes \mathbf{B_2})(\mathbf{A_3} \otimes \mathbf{B_3}) && (30)\\ &= ((\mathbf{A_1 A_2}) \otimes (\mathbf{B_1 B_2}))\,(\mathbf{A_3} \otimes \mathbf{B_3}) \\ &= (\mathbf{A_1 A_2 A_3}) \otimes (\mathbf{B_1 B_2 B_3}) && (31) \end{aligned}$$

From (29) it follows:

$$(\mathbf{I_n} \otimes \mathbf{v})\,\mathbf{v} = (\mathbf{I_n} \otimes \mathbf{v})\,(\mathbf{v} \otimes \mathbf{I_1}) = (\mathbf{I_n v}) \otimes (\mathbf{v I_1}) = \mathbf{v} \otimes \mathbf{v} \tag{32}$$

Moreover, we have the following relation:

$$\begin{aligned} (\mathbf{I_n} \otimes \mathbf{v} \otimes \mathbf{v})\,\mathbf{v} &= (\mathbf{A_n} \otimes \mathbf{v})\,(\mathbf{v} \otimes \mathbf{I_1}) \\ &= (\mathbf{A_n v}) \otimes (\mathbf{v I_1}) \end{aligned} \tag{33}$$

where $\mathbf{A_n} = \mathbf{I_n} \otimes \mathbf{v}$. From (32) it follows $\mathbf{A_n v} = \mathbf{v} \otimes \mathbf{v}$. Finally (33) provides:

$$(\mathbf{I_n} \otimes \mathbf{v} \otimes \mathbf{v})\,\mathbf{v} = \mathbf{v} \otimes \mathbf{v} \otimes \mathbf{v} \tag{34}$$

Unsing $\bigotimes_k \mathbf{v} = \mathbf{v} \otimes ... \otimes \mathbf{v}$, we deduce by recurrence,:

$$\left(\mathbf{I_n} \otimes \bigotimes_{k} \mathbf{v}\right)\mathbf{v} = \bigotimes_{k+1} \mathbf{v} \tag{35}$$

Let us now express the relation between the third order gradient and the third order directional derivative:

$$\begin{aligned} \frac{\partial^3 s}{\partial \mathbf{v}^3}(\mathbf{u}) &= \frac{\partial}{\partial \mathbf{v}}\left[\frac{\partial^2 s}{\partial \mathbf{v}^2}(\mathbf{u})\right]^T = \frac{d}{d\mathbf{u}}\left[\frac{\partial^2 s}{\partial \mathbf{v}^2}(\mathbf{u})\right]^T \mathbf{v} \\ &= \frac{d}{d\mathbf{u}}\left[\mathbf{v}^T \frac{d^2 s}{d\mathbf{u}^2}\mathbf{v}\right]^T \mathbf{v} \\ &= \frac{d}{d\mathbf{u}}\left[\mathbf{v}^T \left(\frac{d^2 s}{d\mathbf{u}^2}\right)^T \mathbf{v}\right]\mathbf{v} \end{aligned} \tag{36}$$

Using Eq. (28), relation (36) can be written:

$$\frac{d}{d\mathbf{u}}\left[\mathbf{v}^T \left(\frac{d^2 s}{d\mathbf{u}^2}\right)^T \mathbf{v}\right]\mathbf{v} = \mathbf{v}^T \frac{d^3 s}{d\mathbf{u}^3}\,(\mathbf{I_n} \otimes \mathbf{v})\,\mathbf{v} \tag{37}$$

Finally (35) and (37) where $k = 1$ give:

$$\frac{\partial^3 s}{\partial \mathbf{v}^3}(\mathbf{u}) = \mathbf{v}^T \frac{d^3 s}{d\mathbf{u}^3}\,(\mathbf{v} \otimes \mathbf{v}) \tag{38}$$

The dimensions are compatible. Let us now compute the forth order derivative:

$$\begin{aligned} \frac{\partial^4 s}{\partial \mathbf{v}^4}(\mathbf{u}) &= \frac{\partial}{\partial \mathbf{v}}\left[\frac{\partial^3 s}{\partial \mathbf{v}^3}(\mathbf{u})\right]^T \\ &= \frac{d}{d\mathbf{u}}\left[\frac{\partial^3 s}{\partial \mathbf{v}^3}(\mathbf{u})\right]^T \mathbf{v} \\ &= \frac{d}{d\mathbf{u}}\left[\mathbf{v}^T \frac{d^3 s}{d\mathbf{u}^3}\mathbf{w}\right]^T \mathbf{v} \\ &= \frac{d}{d\mathbf{u}}\left[\mathbf{w}^T \left(\frac{d^3 s}{d\mathbf{u}^3}\right)^T \mathbf{v}\right]\mathbf{v} \\ &= \mathbf{w}^T \frac{d^4 s}{d\mathbf{u}^4}(\mathbf{I_n} \otimes \mathbf{v})\mathbf{v} \end{aligned} \tag{39}$$

where $\mathbf{w} = \mathbf{v} \otimes \mathbf{v}$. According to (35) and the property $(\mathbf{v} \otimes \mathbf{v})^T = \mathbf{v^T} \otimes \mathbf{v^T}$ Eq. (39) yields:

$$\frac{\partial^4 s}{\partial \mathbf{v}^4}(\mathbf{u}) = (\mathbf{v^T} \otimes \mathbf{v^T}) \frac{d^4 s}{d\mathbf{u}^4}(\mathbf{v} \otimes \mathbf{v}) \tag{40}$$

Eq. (35) yields the following rules by recurrence:

for an even order $k = 2p$:

$$\frac{\partial^k s}{\partial \mathbf{v}^k}(\mathbf{u}) = (\bigotimes_p \mathbf{v^T}) \frac{d^k s}{d\mathbf{u}^k} \bigotimes_p \mathbf{v} \tag{41}$$

for an odd order $k = 2p + 1$:

$$\frac{\partial^k s}{\partial \mathbf{v}^k}(\mathbf{u}) = (\bigotimes_p \mathbf{v^T}) \frac{d^k s}{d\mathbf{u}^k} \bigotimes_{p+1} \mathbf{v} \tag{42}$$

B Proof of the proposition1

Let us multiply the tensors by a $p+q = m+l+1$th Kronecker product of the $\mathbf{n} \times \mathbf{1}$ vector $\mathbf{v}$. Applying Eqs. (30) and (41) yields:

$$\begin{aligned}
&(\bigotimes_{p+q} \mathbf{v^T}) \left(\frac{d^{2p} s}{d\mathbf{u}^{2p}} \otimes \left(\frac{d^{2q} s}{d\mathbf{u}^{2q}} \right)^T \right) \bigotimes_{p+q} \mathbf{v} \\
&= \left((\bigotimes_p \mathbf{v^T}) \otimes (\bigotimes_q \mathbf{v^T}) \right) \left(\frac{d^{2p} s}{d\mathbf{u}^{2p}} \otimes \left(\frac{d^{2q} s}{d\mathbf{u}^{2q}} \right)^T \right) \left(\bigotimes_p \mathbf{v} \otimes \bigotimes_q \mathbf{v} \right) \\
&= \left((\bigotimes_p \mathbf{v^T}) \frac{d^{2p} s}{d\mathbf{u}^{2p}} \bigotimes_p \mathbf{v} \right) \left((\bigotimes_q \mathbf{v^T}) \left(\frac{d^{2q} s}{d\mathbf{u}^{2q}} \right)^T \bigotimes_q \mathbf{v} \right) \\
&= \frac{\partial^{2p} s}{\partial \mathbf{v}^{2p}} \left(\frac{\partial^{2q} s}{\partial \mathbf{v}^{2q}} \right)^T
\end{aligned}$$

In the same manner, applying Eqs. (30) and (42) yields:

$$\begin{aligned}
&(\bigotimes_{m+l+1} \mathbf{v^T}) \left(\frac{d^{2m+1} s}{d\mathbf{u}^{2m+1}} \otimes \left(\frac{d^{2l+1} s}{d\mathbf{u}^{2l+1}} \right)^T \right) \left(\bigotimes_{m+l+1} \mathbf{v} \right) \\
&= \left((\bigotimes_m \mathbf{v^T}) \frac{d^{2m+1} s}{d\mathbf{u}^{2m+1}} \bigotimes_{m+1} \mathbf{v} \right) \left(\bigotimes_{l+1} \mathbf{v^T} \left(\frac{d^{2l+1} s}{d\mathbf{u}^{2l+1}} \right)^T \bigotimes_l \mathbf{v} \right) \\
&= \frac{\partial^{2m+1} s}{\partial \mathbf{v}^{2m+1}} \left(\frac{\partial^{2l+1} s}{\partial \mathbf{v}^{2l+1}} \right)^T
\end{aligned}$$

which completes the proof.

C Computation of the error

Let us consider the n dimensional TKEO which provides the following expression:

$$\Phi_{2,\mathbf{v}}[s(\mathbf{u})] = \mathbf{v}^T \cdot \Psi_2[s(\mathbf{u})] \cdot \mathbf{v} = \frac{\partial s}{\partial \mathbf{v}} \frac{\partial s}{\partial \mathbf{v}} - s \frac{\partial^2 s}{\partial \mathbf{v}^2}$$

Let us consider a general AM-FM signal:

$$s(\mathbf{u}) = A(\mathbf{u}) \cos(\phi(\mathbf{u})) = A(\mathbf{u}) B(\mathbf{u})$$

We will now provide the conditions for which the approximation (43) remains true:

$$\Phi_{2,\mathbf{v}}[s(\mathbf{u})] \simeq A(\mathbf{u})^2 \left(\frac{\partial \phi}{\partial \mathbf{v}}(\mathbf{u})\right)^2 = A(\mathbf{u})^2 \left(\mathbf{w}(\mathbf{u})^T \mathbf{v}\right)^2 \tag{43}$$

The frequency vector is given by:

$$\mathbf{w}(\mathbf{u}) = (w_1(\mathbf{u}), w_2(\mathbf{u}), ..., w_n(\mathbf{u}))^T = \frac{d\phi}{d\mathbf{u}}$$

where:

$$w_i(\mathbf{u}) = \frac{\partial \phi}{\partial x_i}(\mathbf{u})$$

As in (Maragos and Bovik, 1995),(Maragos et al, 1993a), let us consider a band limited envelope $A(\mathbf{u})$, i.e $\mathrm{FT}[A(\mathbf{u})] = \tilde{A}(\boldsymbol{\omega}) = 0$ for $||\boldsymbol{\omega}|| \geq \omega_A$ where FT[] is the Fourier Transform. Giving a mean spectral absolute value:

$$\mu_A = \frac{1}{(2\pi)^n} \int_{-\omega_A}^{+\omega_A} ... \int_{-\omega_A}^{+\omega_A} \left|\tilde{A}(\boldsymbol{\omega})\right| d\omega_1 d\omega_2 ... d\omega_n \tag{44}$$

we deduce the following relations for any partial derivatives giving $r = r_1 + r_2 + ... + r_n$:

$$\mathrm{FT}\left[\frac{\partial^r A}{\partial x_1^{r_1} \partial x_2^{r_2} ... \partial x_n^{r_n}}\right] = (j\omega_1)^{r_1} (j\omega_2)^{r_2} ... (j\omega_n)^{r_n} \tilde{A}(\boldsymbol{\omega})$$

$$\Rightarrow \left|\frac{\partial^r A}{\partial x_1^{r_1} \partial x_2^{r_2} ... \partial x_n^{r_n}}\right| = \left|\mathrm{FT}^{-1}\left[(j\omega_1)^{r_1} (j\omega_2)^{r_2} ... (j\omega_n)^{r_n} \tilde{A}(\boldsymbol{\omega})\right]\right| \leq \omega_A^r \mu_A$$

Moreover, the quantity $\frac{\partial^r A}{\partial x_1^{r_1} \partial x_2^{r_2} ... \partial x_n^{r_n}}$ being the general term of the higher order gradient $\frac{d^r A}{d\mathbf{u}^r}$, it follows from (45), and the results (41),(42) obtained in appendix B linking the higher order gradients and directional derivatives :

for an even order $r = 2p$:

$$\left|\frac{\partial^r A}{\partial \mathbf{v}^r}(\mathbf{u})\right| \leq n^r \omega_A^r \mu_A ||\bigotimes_p \mathbf{v}^T|| \cdot ||\bigotimes_p \mathbf{v}|| \tag{45}$$

for an odd order $r = 2p + 1$:

$$\left|\frac{\partial^r A}{\partial \mathbf{v}^r}(\mathbf{u})\right| \leq n^r \omega_A^r \mu_A ||\bigotimes_p \mathbf{v}^T|| \cdot ||\bigotimes_{(p+1)} \mathbf{v}|| \tag{46}$$

Moreover, the following result is deduced from the properties of the Kronecker product, provided that the dimensions are compatible:

$$(A_1 \otimes A_2 \otimes ... \otimes A_n)(B_1 \otimes B_2 \otimes ... \otimes B_n) = (A_1 B_1) \otimes (A_2 B_2) \otimes ... \otimes (A_n B_n) \tag{47}$$

Eq. (47) yields:

$$\begin{aligned} ||\bigotimes_p \mathbf{v}||^2 &= \bigotimes_p \mathbf{v} \left(\bigotimes_p \mathbf{v}\right)^T = \bigotimes_p \mathbf{v} \bigotimes_p \mathbf{v}^T \\ &= (\mathbf{v}\mathbf{v}^\mathbf{T}) \otimes (\mathbf{v}\mathbf{v}^\mathbf{T}) \otimes ... \otimes (\mathbf{v}\mathbf{v}^\mathbf{T}) \\ &= ||\mathbf{v}||^2 \otimes ||\mathbf{v}||^2 \otimes ... \otimes ||\mathbf{v}||^2 \\ &= ||\mathbf{v}||^{2p} \end{aligned} \tag{48}$$

Finally:

$$||\bigotimes_p \mathbf{v}|| = ||\mathbf{v}||^p \tag{49}$$

Thus Eqs. (45),(46) and (49) provide for any order r:

$$\left|\frac{\partial^r A}{\partial \mathbf{v}^r}(\mathbf{u})\right| \leq n^r \mu_A \omega_A^r ||\mathbf{v}||^r \tag{50}$$

Let us express now the first and second order directional derivatives of $A(\mathbf{u})$ according to a normalized vector $||\mathbf{v}|| = 1$:

$$\left|\frac{\partial A}{\partial \mathbf{v}}(\mathbf{u})\right| \leq n\omega_A \mu_A \qquad \left|\frac{\partial^2 A}{\partial \mathbf{v}^2}(\mathbf{u})\right| \leq n^2 \omega_A^2 \mu_A \tag{51}$$

Finally, it is possible to deduce the following inequality:

$$|\Phi_{2,\mathbf{v}}[A(u)]| \leq n^2 \omega_A^2 \mu_A^2 + n^2 \omega_A^2 \mu_A A_{\max} \tag{52}$$

In order to process narrow band signals, we now express each local component frequency as a sum of a constant carrier term and an excursion frequency:

$$w_i(\mathbf{u}) = w_{c,i} + w_{m,i} f_i(\mathbf{u})$$

As in (Maragos and Bovik, 1995), we assume that $f_i(\mathbf{u}) \in [-1, +1]$ and $w_{m,i}$ is the maximum deviation of the frequency from its center value $0 \leq w_{m,i} \ll |w_{c,i}|$. Let us now compute the higher order derivatives of $B(\mathbf{u}) = \cos(\phi(\mathbf{u}))$ according to the vector $\mathbf{v}$

$$\frac{\partial B}{\partial \mathbf{v}} = \frac{\partial \phi}{\partial \mathbf{v}} \sin(\phi(\mathbf{u})) \tag{53}$$

$$\frac{\partial^2 B}{\partial \mathbf{v}^2} = \frac{\partial^2 \phi}{\partial \mathbf{v}^2} \sin(\phi(\mathbf{u})) - \left(\frac{\partial \phi}{\partial \mathbf{v}}\right)^2 \cos(\phi(\mathbf{u})) \tag{54}$$

We suppose that the excursion $\Delta_i j = w_{m,i} f_i(\mathbf{u})$, for all i is such that $f_i(\mathbf{u})$, is a band limited signal i.e, $\mathrm{FT}[f_i(\mathbf{u})] = \tilde{f}_i(\boldsymbol{\omega}) = 0$ for $||\boldsymbol{\omega}|| \geq \omega_{f_i}$. We suppose that $\omega_{f_i} \leq \omega_{c_i}$ where $\omega_c = ||\mathbf{w_c}(\mathbf{u})||$ corresponds to the norm of the local central frequency, which means that the frequency excursion is not too fast. Let us give a mean spectral absolute value:

$$\mu_{f_i} = \frac{1}{(2\pi)^n} \int_{-\omega_{f_i}}^{+\omega_{f_i}} \ldots \int_{-\omega_{f_i}}^{+\omega_{f_i}} \left|\tilde{f}_i(\boldsymbol{\omega})\right| d\omega_1 d\omega_2 \ldots d\omega_n$$

Let us compute the second order derivative along a normalized vector $\mathbf{v} = (v_1, \ldots, v_n)^T$:

$$\frac{\partial^2 \phi}{\partial \mathbf{v}^2}(\mathbf{u}) = \mathbf{v}^T \frac{d^2 \Phi}{d\mathbf{u}^2} \mathbf{v} = \sum_{i=1}^{n} \sum_{j=1}^{n} v_i w_{m_i} \frac{\partial f_i}{\partial x_j} v_j \tag{55}$$

A similar inequality as Eq. (45) and the previous conditions lead to:

$$\left|\frac{\partial^2 \phi}{\partial \mathbf{v}^2}(\mathbf{u})\right| \ll \sum_{i=1}^{n} \sum_{j=1}^{n} w_{c_i}^2 \mu_{f_i} \tag{56}$$

The choice of $\mu_{f_i} \simeq 1$ means that the FT of the functions f_i own linear phases (Maragos et al, 1993a). Then, the inequality (56) becomes:

$$\left|\frac{\partial^2 \phi}{\partial \mathbf{v}^2}(\mathbf{u})\right| \ll \sum_{i=1}^{n} \sum_{j=1}^{n} w_{c_i}^2 = n\omega_c^2 \tag{57}$$

On the other hand, an appropriate choice of the vector $\mathbf{v}$ leads to:

$$\frac{\partial \phi}{\partial \mathbf{v}}(\mathbf{u}) = \frac{d\Phi}{d\mathbf{u}} \mathbf{v} \geq ||\mathbf{w}(\mathbf{u})|| \simeq w_c \tag{58}$$

For example the following vector used in our study, satisfies (58):

$$\mathbf{v} = \left(\frac{\text{sign}(w_1)}{\sqrt{n}}, ..., \frac{\text{sign}(w_n)}{\sqrt{n}} \right)^T$$

Finally, it is trivial to generalize the well known property of the application of the TKEO to the product of functions, regarding the directional derivatives:

$$\begin{aligned} \Phi_{2,\mathbf{v}}[A(\mathbf{u})B(\mathbf{u})] &= A^2(\mathbf{u})\Phi_{2,\mathbf{v}}[B(\mathbf{u})] + B^2(\mathbf{u})\Phi_{2,\mathbf{v}}[A(\mathbf{u})] \\ &= A^2(\mathbf{u}) \left(\left(\frac{\partial \phi}{\partial \mathbf{v}} \right)^2 - \frac{1}{2} \frac{\partial^2 \phi}{\partial \mathbf{v}^2} \sin 2\phi(\mathbf{u}) \right) + \Phi_{2,\mathbf{v}}[A(\mathbf{u})] \cos \phi(\mathbf{u}) \end{aligned} \quad (59)$$

According to our hypothesis, the instantaneous envelope $A(\mathbf{u})$ is a slow signal, relatively to the carrier one, which implies that $\omega_A \ll \omega_c$. Moreover, the envelope being observed on a short time interval, it is possible to extrapolate it as a sinusoidal function i.e, $\mu_A \simeq A_{\max}$. Then the equality (59) yields:

$$\Phi_{2,\mathbf{v}}[A(\mathbf{u})B(\mathbf{u})] = A^2(\mathbf{u}) \left(\frac{\partial \phi}{\partial \mathbf{v}} \right)^2 + \varepsilon_{\mathbf{v}}(\mathbf{u}) \quad (60)$$

According to Eqs. (52) and (57) and the previous assumptions, the error term $\varepsilon_{\mathbf{v}}$ verifies:

$$|\varepsilon_{\mathbf{v}}(\mathbf{u})| \ll A^2_{\max} \left(\frac{1}{2} n \omega_c^2 + 2n^2 \omega_c^2 \right)$$

When comparing with the bound of the error detailed in (Maragos and Bovik, 1995), there is a multiplicative factor n. In general, for any vector $\mathbf{v}$ the operator leads to:

$$\begin{aligned} \Phi_{2,\mathbf{v}}[A(\mathbf{u}) \cos \phi(\mathbf{u})] = A^2(\mathbf{u}) &\left(\left(\frac{\partial \phi}{\partial \mathbf{v}} \right)^2 - \mathbf{v}^T \frac{1}{2} \frac{d^2 \phi}{d\mathbf{u}^2} \sin 2\phi(\mathbf{u}) \mathbf{v} \right) \\ &+ \mathbf{v}^T \Psi_{2,\mathbf{v}}[A(\mathbf{u})] \cos \phi(\mathbf{u}) \mathbf{v} \end{aligned} \quad (61)$$

Notice tha it is possible to find a theoretical vector which minimizes the error term and provides an energy operator proportional to the quantity $A(\mathbf{u})||w(\mathbf{u})||^2$. This corresponds to a classical constrainst minimization problem i.e:

$$\begin{aligned} &\text{minimize} \quad \mathbf{v}^T \mathbf{R} \mathbf{v} \quad \text{subject to} \quad \mathbf{v}^T \mathbf{w} = ||\mathbf{w}|| \\ &\text{where :} \quad \mathbf{R} = \frac{1}{2} \frac{d^2 \phi}{d\mathbf{u}^2} + \Psi_{2,\mathbf{v}}[A(\mathbf{u})] \end{aligned}$$

Provided that the matrix $\mathbf{R}$ is not a singular one, a solution to this problem is given by:

$$\mathbf{v} = \frac{\mathbf{R}^{-1}\mathbf{w}}{\mathbf{w}^T \mathbf{R}^{-1} \mathbf{w}} ||\mathbf{w}||$$

Considering a slow varying envelope in a short time interval, the optimal vector depends on the Hessian of the phase and the frequency.

Acknowledgements The authors would like to thank P. Montgomery of the Iness laboratory for providing the interferometric image.

References

Boudraa A, Salzenstein F, Cexus J (2005) Two-dimensional continuous higher-order energy operators. Optical Engineering 44(11):7001–7010

Boudraa A, Bouchikhi A, Diop E (2008) Teager-kaiser energy bi-level thresholding. In: IEEE International Symposium on Communications, Control and Signal Processing, Malta, pp 1086–1090

Bovik A, Gopal N, Emmoth T, Restrepo A (1992) Localized measurement of emergent image frequencies by gabor wavelets. IEEE Trans Info Theory 38(2):691–712

Brewer J (1978) Kronecker products and matrix calculus in system theory. IEEE Trans Circuits and Systems 25(9):772–781

Cai QW, Wei P, Xiao X (2010) Single-channel blind separation of overlapped multicomponents based on energy operator. SCIENCE CHINA Information Sciences 53(1):147–157

Diop E, Boudraa A, Bouchikhi A (2008) Image contrast enhancement based on 2d teager-kaiser operator. In: IEEE International Conference on Image Processing, San Diego, USA, pp 3180–3183

Felsberg M, Granlund G (2004) POI detection using channel clustering and the 2D energy tensor. In: Pattern Recognition: 26th DAGM Symposium, Springer Berlin, Tübingen, Germany, LNCS, vol 3175, pp 103–110

Felsberg M, Jonsson E (2005) Energy tensors: Quadratic phase invariant image operators. In: DAGM 2005, Springer, LNCS, vol 3663, pp 493–500

Felsberg M, Köthe U (2005) Get: The connection between monogenic scale-space and gaussian derivatives. In: Kimmel R, Sochen N, Weickert J (eds) Scale Space and PDE Mathods in Computer Vision, Springer, LNCS, vol 3459, pp 192–203

Havlicek J, Tay P, Bovik A (2005) Handbook of Image and Video Processing, 2nd edn, Elsevier Academic Press, Burlington, chap AM-FM image models: fundamental techniques and emerging trends, pp 377–395

Kaiser J (1990) On a simple algorithm to calculate the energy of a signal. In: Proc. ICASSP, pp 381–384

Larkin K (1996) Efficient nonlinear algorithm for envelope detection in white light interferometry. Journal of Optical Society of America A 13:832–843

Larkin K (2005) Uniform estimation of orientation using local and nonlocal 2-d energy operators. Optics Express 13(20):8097–8121

Maragos P, Bovik A (1995) Image demodulation using multidimensional energy separation. J Opt Soc Am A 12:1867–1876

Maragos P, Potamianos A (1995) Higher order differential energy operators. IEEE Sig Proc Letters 2:152–154

Maragos P, Kaiser J, Quatieri T (1993a) On amplitude and frequency demodulation using energy operators. IEEE Trans Signal Processing 41(4):1532–1550

Maragos P, Quatieri T, Kaiser J (1993b) Energy separaton in signal modulations with applications to speech analysis. IEEE Trans Signal Processing 41:3024–3051

Mitra S, Li H, Lin I, Yu T (1991) A new class of nonlinear filters for image enhancement. In: Proc. ICASSP, vol 91, pp 2525–2528

Moon TK, Stirling WC (2000) Mathematical Methods and Algorithms for Signal Processing. Prentice Hall, Upper Saddle River, NJ

Ramponi G, Strobel N, Mitra S, Yu T (1996) Nonlinear unsharp masking methods for image contrast enhancement. Journal of Electronic Imaging 5(3):353–366

Salzenstein F, Boudraa A (2009) Multi-dimensional higher order differential operators derived from the Teager-kaiser energy tracking function. Signal Processing 89(4):623–640

Salzenstein F, Montgomery P, Montaner D, Boudraa A (2005) Teager-kaiser energy and higher order operators in white light interference microscopy for surface shape measurement. EURASIP J Appl Signal Process 17:2804–2815

Salzenstein F, Boudraa A, Cexus J (2007) Generalized higher-order nonlinear energy operators. J Opt Soc Am A 24:3717–3727

Vakman D (1996) On the analytic signal, the teager-kaiser energy algorithm, and other methods for defining amplitude and frequency. IEEE Trans Signal Proc 44(4):791–797

Vetter WJ (1973) Matrix calculus operations and taylor expansions. SIAM review 15(2):352–369

Vleesschauwer DD, Cheikh FA, Hamila R, Gabbouj M (1997) Watershed segmentation of image enhanced by teager energy driven diffusion. In: Proc. Sixth Conf. Image processing and its applications, pp 254–258

Yu T, Mitra S, Kaiser J (1991) A novel nonlinear filter for image enhancement. In: Proc. SPIE/SPSE Sym. on Electronic Imaging: Science and Technology, pp 303–309